

Wideband Reconfigurable Millimeter-Wave Linear Array Antenna Using Liquid Crystal for 5G Networks

Ali El Hajj Hassan^{1,2}, Najib Fadlallah¹, Mohammad Rammal¹, Georges Zakka El Nashef², Elias Rachid²

¹Ecole Doctorale des Sciences et de la Technologie (EDST), Lebanese University (LU), Beirut, Lebanon

²Ecole Supérieure d'Ingénieurs de Beyrouth (ESIB), Université Saint-Joseph (USJ), Beirut, Lebanon

Email: ali.hajj hassam@net.usj.edu.lb, n_fadlallah@yahoo.com, m_rammal@hotmail.com, georges.nashef24@gmail.com, Elias.rachid@usj.edu.lb

How to cite this paper: El Hajj Hassan, A., Fadlallah, N., Rammal, M., El Nashef, G.Z. and Rachid, E. (2021) Wideband Reconfigurable Millimeter-Wave Linear Array Antenna Using Liquid Crystal for 5G Networks. *Wireless Engineering and Technology*, 12, 1-14.

<https://doi.org/10.4236/wet.2021.121001>

Received: January 8, 2021

Accepted: January 26, 2021

Published: January 29, 2021

Copyright © 2021 by author(s) and Scientific Research Publishing Inc. This work is licensed under the Creative Commons Attribution International License (CC BY 4.0).

<http://creativecommons.org/licenses/by/4.0/>



Open Access

Abstract

The advanced design of a 10×1 linear antenna array system with the capability of frequency tunability using GT3-23001 liquid crystal (LC) is proposed. The design for this reconfigurable wideband antenna array for 5G applications at Ka-band millimeter-wave (mmw) consists of a double layer of stacked patch antenna with aperture coupled feeding. The bias voltage over LC varies from 0 V to 10.6 V to achieve a frequency tunability of 1.18 GHz. The array operates from 25.3 GHz to 33.8 GHz with a peak gain of 19.2 dB and a beamwidth of 5.2° at 30 GHz. The proposed reconfigurable antenna array represents a real and efficient solution for the recent and future mmw 5G networks. The proposed antenna is suitable for 5G base stations in stadiums, malls and convention centers. It is proper for satellite communications and radars at mmw.

Keywords

5G Networks, Liquid Antenna, Liquid Crystal, Frequency Reconfigurability, Antenna Array, Millimeter-Wave

1. Introduction

Five Generation (5G) networks are expected to bring a principal resolution for the extremely aggregated demand of wide bandwidth and moderate mobile data traffic. The recent wireless communication technologies ability and capability challenge many critical limitations. However, as the low-frequency range is fully loaded and incapable to fulfill the necessary wide bandwidth for future 5G ap-

plications, many international organizations have licensed or recommended mmw spectrum as an efficient operating frequency band for 5G standards [1] including 24, 28, 37, 39, and 60 GHz. Besides, The US Federal Communications Commission (FCC) has suggested 28 GHz and 38 GHz bands for 5G standards, while the UK Office of Communications (OfCom) has established 5G bands on 26 GHz [2]. As well, amongst the mmw spectra, Ka-band represents one of the effective suggested band for 5G wireless communication technologies due to its wider bandwidth, miniaturized devices, lower absorptions, less path loss and delays, suitability for multipath environments and reduced signal vanishing like weather attenuations and rain fades [3] [4].

The reconfigurable mmw antennas are expected to be the principal pivot for the 5G and next generation wireless networks. The future development of mobile communication will depend on the development of novel techniques, technologies, and topologies for the design of reconfigurable mmw antennas. That fact will initiate for improving the future antenna over increasing the bandwidth, tuning the operating frequency, and minimizing the antenna size. Pin diodes [5], varactors [6], capacitors [7], variable resistors [8], inductors and transformers [9], RF MEMS [10], and LCs [11] [12] have been integrated in several described antenna designs to attain frequency reconfiguration.

In the previous years and the upcoming future, the tunable mmw components based on LC materials are of collective interest in research and industry. The LCs can be used only in the nematic phase for designing electronically tunable RF, microwave, and mmw devices. The use of LCs in mmw devices represents a novel method for achieving frequency agility or pattern and polarization reconfigurability and multi-functional tunability [13]. These tunable anisotropic materials have been targeted in the last few years for the design of reconfigurable antennas [14] [15], resonators [16], phase shifters [17], and filters [18]. An anisotropy material is characterized by a permittivity tensor. Thus, the anisotropy is typically assumed to present a variable effective permittivity (ϵ_{eff}) to the electromagnetic wave [19]. The dielectric permittivity tensor of an LC can be controlled by a low biasing voltage where its molecules tend to be oriented in the direction of the applied electrostatic field [20].

High directivity, high gain, and narrow beamwidth are essential concerns while designing mmw antennas for a 5G wireless systems. However, the single antenna had typically low gain due to the configuration. Therefore, another good solution to compensate for the high propagation loss related to mmw bands is to use high gain antenna arrays for 5G mobile network comprising a narrower radiation beam [21]. Recent studies have reported several reconfigurable mmw antenna array designs for 5G wireless applications in order to enhance channel capacity and spectral efficiency and minimize weather attenuations [22] [23] [24] [25].

In this article, an optimized design of a 10×1 linear 5G wideband frequency reconfigurable stacked patch antenna array based on GT3-23001 LC attaining an operating frequency range from 25.3 GHz to 33.8 GHz with an antenna array

gain of more than 17.4 dB is presented. Detailed parameter variations of the square patch width and the height of the Rohacell layer result in optimized mutual resonances of the array elements and the coupling aperture. Accordingly, an array antenna with an optimized impedance bandwidth and a looked-for high gain is studied, simulated, and optimized in 3D with CST Microwave Studio 2016.

The article is organized as following: Configurations of the single antenna and antenna array are indicated in Section-II. The simulated results are presented and discussed in Section-III. The conclusion is the Section-IV.

2. Research Method

2.1. Single Patch Antenna Configuration

One of patch antenna key advantages is that these planar antennas are small in size, robust in mechanics, cheap in production and suitable for antenna arrays design. However, the patch antennas face-up the challenge of narrow bandwidth. The proposed design in this work deals with a complex design of 3 technical steps built on the simple patch antenna design to achieve the current and upcoming requirements of 5G networks. The need for wide bandwidth and high gain for the proposed design impose these 3 technical steps which are the multi-layer stacked patch assembly, the frequency reconfigurability process based on controlling the variable permittivity of GT3-23001 LC anisotropic material through a variable bias voltage, and the aperture coupled feeding. This external bias voltage changes the orientation of the LC molecules inside a cavity below the first metallic patch as shown in **Figure 1**. In consequence, that affects the variable permittivity of the LC material.

The developed single antenna design is an advanced and optimized design of the compact reconfigurable stacked patch antenna presented in our previous work described in [26] to provide the planned bandwidth and antenna gain, and enhancing the front to back ratio of the main lobe and the tunability over frequency. The compact reconfigurable antenna design for 5G mmw applications in [26] consists of two stacked square patch antenna using aperture coupled feeding. A GT3-23001 LC square cavity is drilled in the first patch antenna's substrate. The Rogers RO-3003 material with $\epsilon_r = 3$ and $\tan\delta = 0.001$ is used as a dielectric substrate in 3 layers for twice patch antennas and feed. An intermediate layer of Rohacell 31 IG/A with dielectric constant $\epsilon_r = 1.05$ and loss tangent $\tan\delta = 0.0034$ [27] is located between the patch antennas layers. The dimensions of the described antenna are $(5.34 \times 5.34 \times 2.06) \text{ mm}^3$.

After a parametric study on the height of the Rohacell layer and the width of the two patch antennas' substrate and feed, an advanced design of wideband frequency reconfigurable stacked patch antenna with a high gain was developed. The designed structure keeps the topology of the antenna designated in [26] with two adjustments by reducing the height of the Rohacell layer from 1 mm to 0.75 mm, and enlarging the width of the patch antennas' substrate from half wavelength

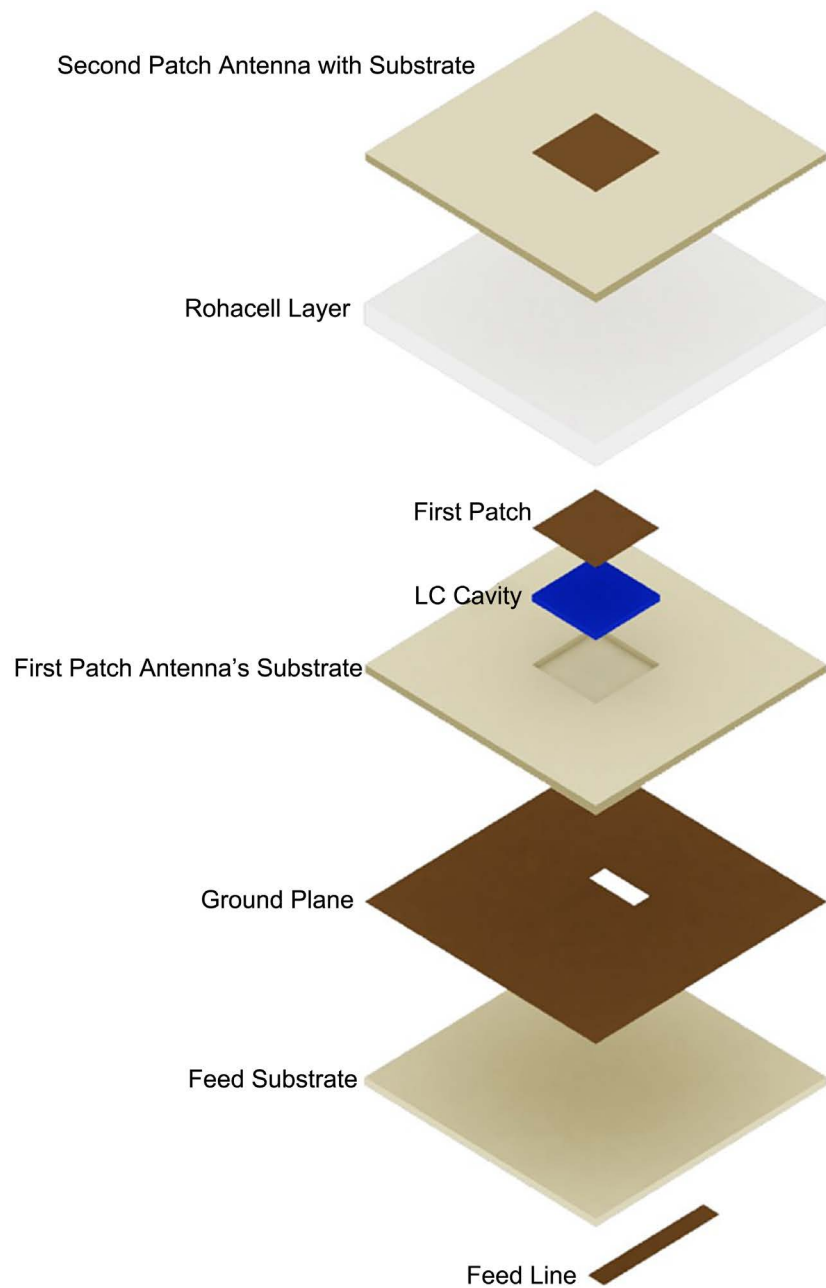


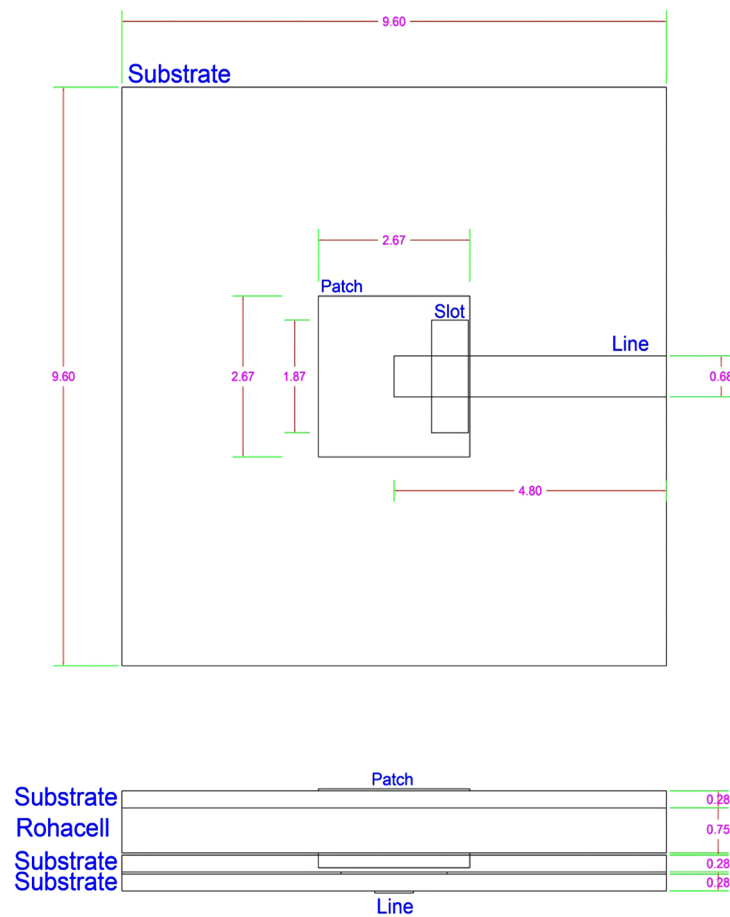
Figure 1. The structure over layers of the developed single stacked patch antenna.

5.34 mm over the center frequency 28 GHz to 0.9 of the specified wavelength 9.6 mm. The structure of the designed single antenna is presented in **Figure 1**. The thickness of the metallic part of the patches, ground plane, and the feed line is equal to 0.035 mm. Moreover, the width and length of the ground plane are the same as the substrates and the Rohacell layer.

The developed single antenna parameters' dimensions of substrates, the patches, LC's square LC cavity, Rohacell layer, feed line, and slot over the ground plane are shown in **Figure 2** and listed in **Table 1**. The dimensions of the stacked patch antenna are $(9.6 \times 5.34 \times 1.31) \text{ mm}^3$.

Table 1. The optimized parameters' dimensions of the proposed antenna.

Parameters	Dimensions (mm)
Substrate Width	9.6
Substrate Length	9.6
Substrate Height	0.28
Patch Width	2.67
Patch Length	2.67
LC Width	2.67
LC Height	0.21
Rohacell Height	0.75
Feed Line Width	0.68
Feed Line Length	4.8
Feed Slot Width	0.65
Feed Slot Length	1.87

**Figure 2.** The top and front views of the developed single stacked patch antenna.

2.2. Antenna Array Configuration

The linear 10×1 array antenna is composed of 20 square patch antennas alternatively arranged in horizontal and vertical configurations as shown in **Figure 2** and **Figure 3**. A Rohacell layer is sandwiched by 2 different layers of square

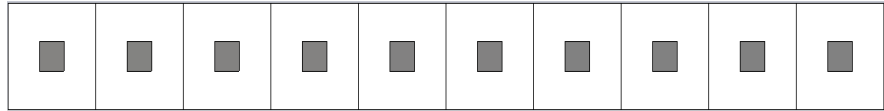


Figure 3. The configuration of the 10×1 linear stacked patch antenna array.

patch antennas where each one contains 10 elements. The linear array antenna is fed by a series of aperture coupled feeding. Further, a GT3-23001 LC is used to provide continuous frequency tunability via controlling the bias voltage. The dimensions of the linear stacked patch antenna array are $(96 \times 5.34 \times 1.31)$ mm³.

3. Results and Analysis

The compact reconfigurable stacked patch antenna described in [26] operates at a frequency range from 25.4 GHz to 33.5 GHz with a bandwidth of 8.16 GHz (27.7%) and a maximum antenna gain of 6.75 dB for a controlling bias voltage of 0 V. The frequency shift achieves 1.15 GHz based on the variation of the bias voltages over GT3-23001 LC. **Figure 4** and **Figure 5** show respectively the results of the return loss characteristics and maximum gain versus frequency of the antenna cited in [26] for 3 different bias voltages at 0 V, 4.42 V, and 10.6 V.

The single stacked patch antenna developed in this work is matched to operate in a frequency range from 25.2 GHz to 33.9 GHz with a wide bandwidth of 8.65 GHz and corresponding to 29.3% of the center frequency, as shown in **Figure 6**. The use of GT3-23001 LC as a dielectric anisotropic material controlled by bias voltages imposes a frequency shift of 1.18 GHz.

The maximum gains for the main lobes of the developed single antenna over the operational frequency range and bias voltage are presented in **Figure 7**. For a bias voltage of 0 V, the maximum gain values of the antenna vary between 7.75 dB at 25 GHz and 8.7 dB at 31 GHz. Also, **Figure 7** shows up an interesting result which is the shift of the maximum gain values over frequencies by variation of the bias voltages.

The compact reconfigurable wideband antenna based on GT3-23001 LC described in [26] operates at mmw from 25.4 GHz to 33.5 GHz with a bandwidth of 8.16 GHz and a maximum antenna gain of 6.75 dB is achieved. **Figure 8** represents a comparison over the radiation pattern of the developed antenna and the compact antenna reported in [26] at 30 GHz and for azimuth angle (φ) = 0°. The developed antenna design shows improvements over the radiation pattern compared to the other antenna design. For the proposed antenna in this work, the maximum gain on the main lobe is equal to 8.5 dB versus 6.75 dB to the compared antenna. As well, the front to back ratio indicates a respectable enhancement for -16.9 dB against -7.5 dB. Also, the main lobe angular beamwidth at 3 dB (θ_{3dB}) achieves 76.5° for the proposed antenna and 83.7° for the compared one.

The variations of the return loss (S_{11}) parameters of the proposed reconfigurable antenna array using GT3-23001 LC by varying the bias voltage are plotted in **Figure 9**. The antenna array operates from 25.2 GHz to 33.8 GHz with a bandwidth

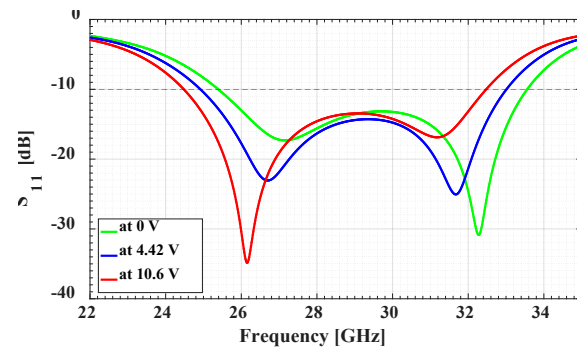


Figure 4. Return loss S_{11} of the compact antenna over the bias voltages.

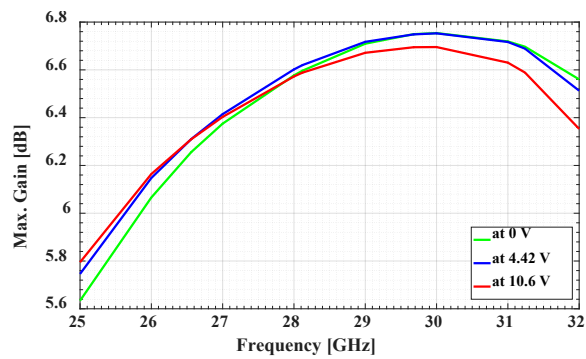


Figure 5. Maximum gain of the compact antenna over the bias voltages.

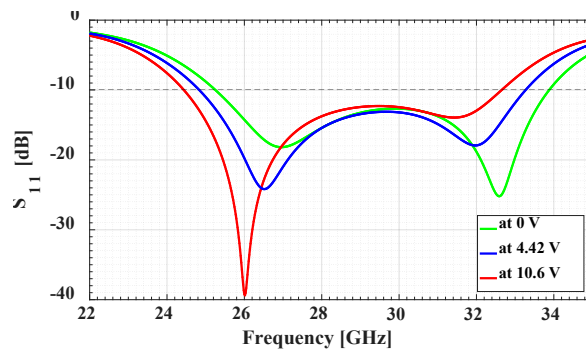


Figure 6. Return loss S_{11} of the developed single antenna over the bias voltages.

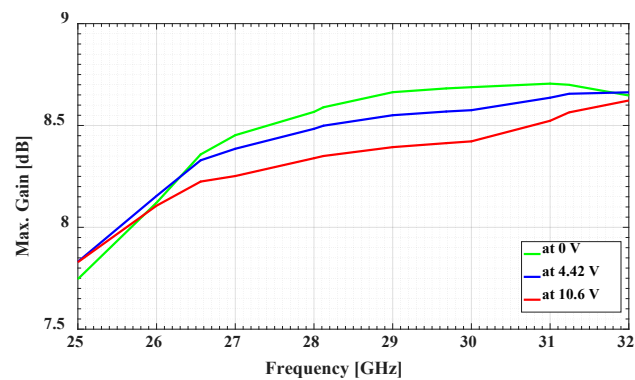


Figure 7. Maximum gain of the developed single antenna over the bias voltages.

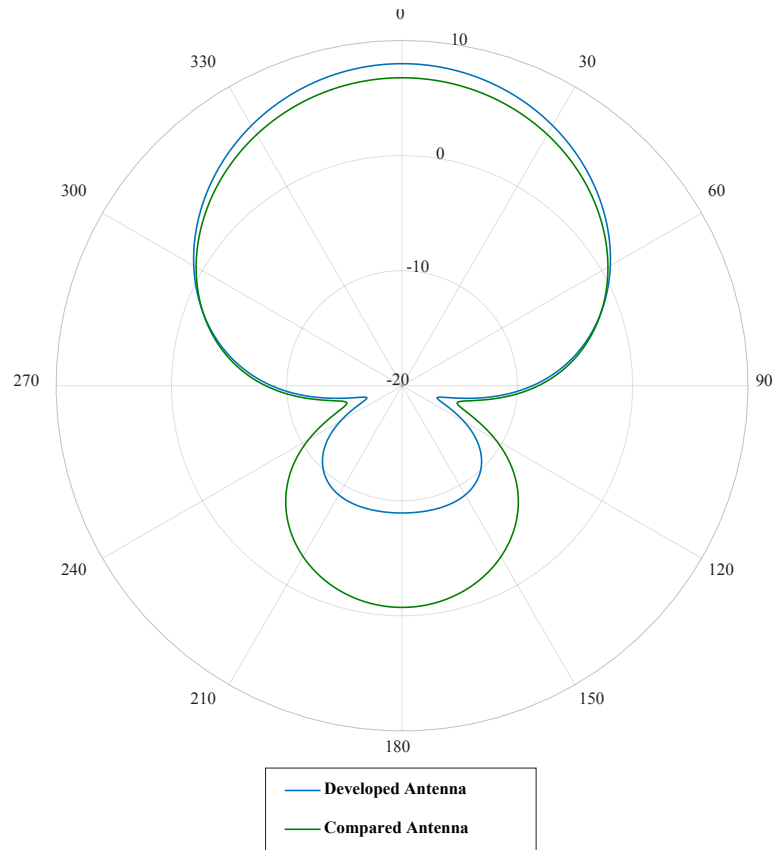


Figure 8. Radiation patterns of the developed single patch antenna and the compared compact patch antenna at 30 GHz.

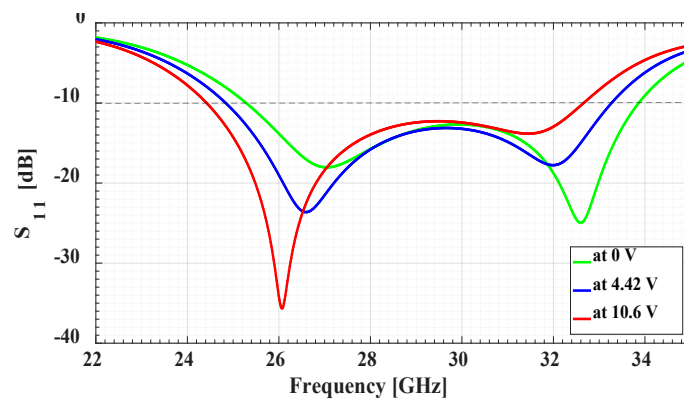


Figure 9. Return loss S_{11} of the proposed antenna array over the bias voltages.

of 8.6 GHz and a frequency shift of 1.15 GHz. **Figure 10** shows that the mutual coupling at controlling bias voltage 0 V and 10.6 V is under -24.5 dB and 24 dB respectively, which provide a respectable isolation between the adjacent array elements.

The radiation patterns of the proposed antenna array for 28 GHz and 30 GHz over 0 V bias voltage and for $\varphi = 0^\circ$ are plotted in **Figure 11**. The radiation pattern at 28 GHz provides a maximum gain on the main lobe of 18.6 dB with a

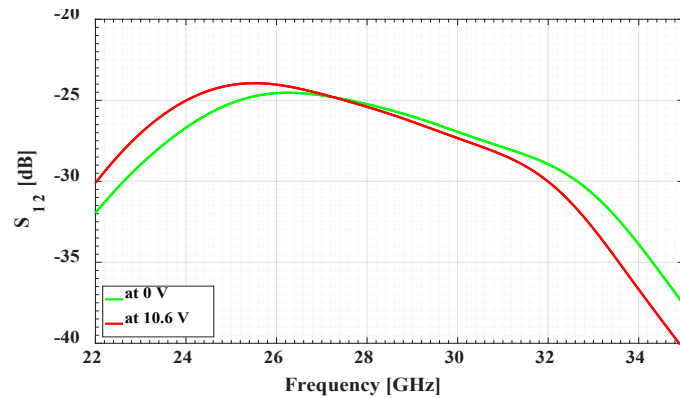


Figure 10. Isolation S_{12} of the proposed antenna array over the bias voltages.

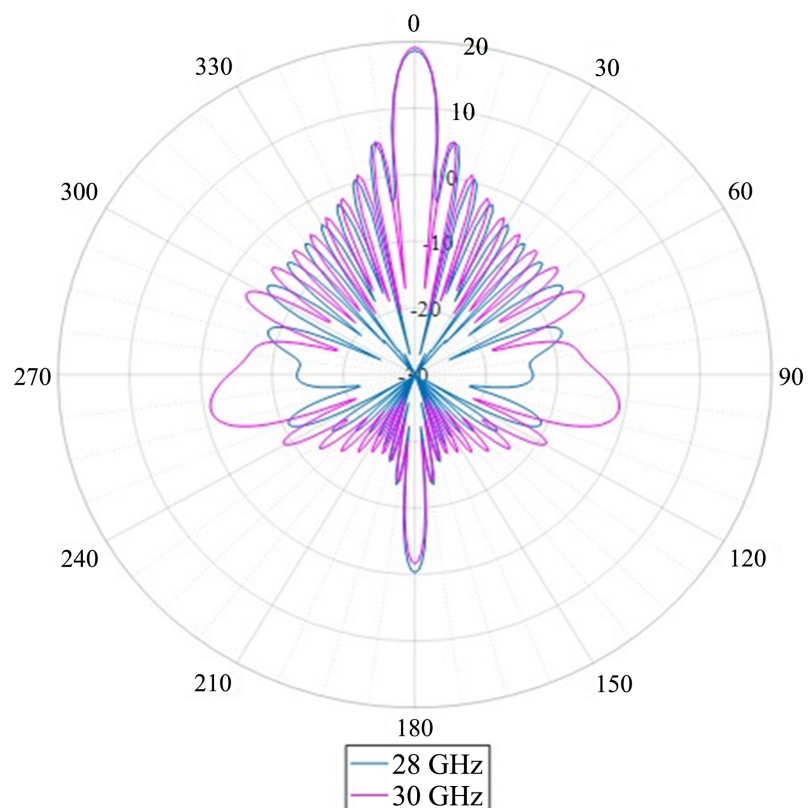


Figure 11. Radiation patterns of the proposed antenna array for 28 GHz and 30 GHz over 0 V bias voltage.

front to back ratio of 18.1 dB and an angular width 5.7° . On the other side, the radiation pattern at 30 GHz achieves a maximum gain on the main lobe of 19.2 dB with a front to back ratio of 21.2 dB and an angular beamwidth of 5.2° . Over the operational frequency range, the maximum gain on the main lobe varies from 17.4 dB to 19.2 dB. The $\theta_{3\text{dB}}$ at 3 dB and for plane $\varphi = 0^\circ$ decreases from 6.3° to 4.8° when the frequency increases from 25.2 GHz to 33.8 GHz.

The results plotted in **Figure 12** and **Figure 13** present the radiation efficiency and the total efficiency of the linear reconfigurable antenna array respectively for

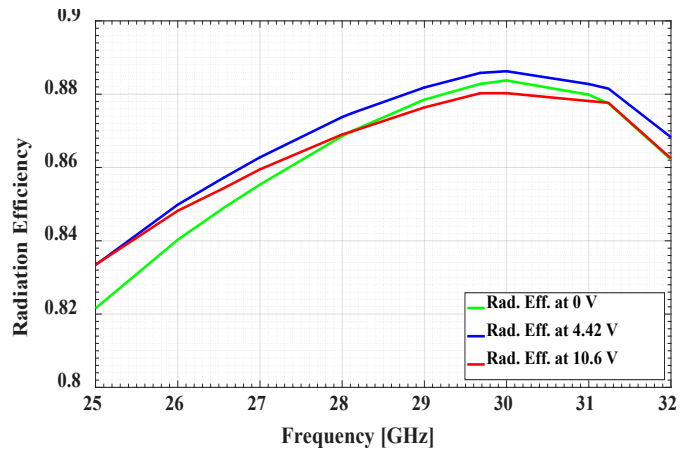


Figure 12. Radiation efficiency of the proposed antenna array over the bias voltages.

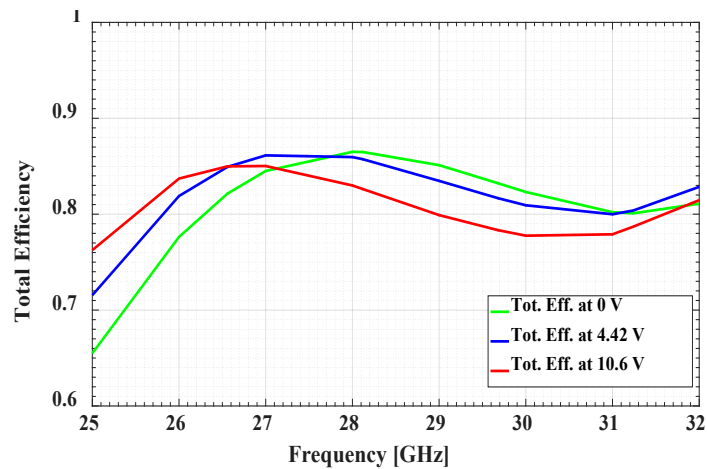


Figure 13. Total efficiency of the proposed antenna array over the bias voltages.

the bias voltages. The total efficiency is around 80% all-over the frequency range and for the different bias voltage. Thus, the proposed antenna array has a suitable efficiency. Suitable antenna efficiency means an effective radiated power for this antenna design.

To clarify additionally the quality of the proposed antenna's design and results, a comparison based on several recent antenna array design parameters for mmw 5G applications is presented. A dual-function connected slot antenna array (CSAA) based on different varactors operates in the frequency range 23 GHz to 29 GHz with a maximum gain of 12.5 dBi [28]. Additional, wideband printed array clutched by LTE-a 4 × 4 MIMO antennas is proposed with a bandwidth of 2 GHz, a maximum gain of 9 dB, and radiation efficiency about 75% [29]. The reconfigurable antenna array based on switching two PIN-diode shows a frequency operating band from 27.2 GHz to 28.35 GHz with a maximum gain of about 6 dBi and a radiation efficiency of around 51% over the bandwidth [30]. Other, multiband dual-standard MIMO antenna system based on monopoles and connected slots with a bandwidth of 4.8 GHz and a maximum gain of 9.9 dB

is achieved [31]. Further, a compact MIMO antenna integrated with an array antenna is reported with a bandwidth of 2.4 GHz and a maximum gain of 8.2 dB [32]. The maximum gain, bandwidth, or radiation efficiency and tunability of the pre-listed works in [28] [29] [30] [31] [32] did not reach the results that the proposed design for all or some of these parameters.

Moreover, the antenna array at mmw band for 5G applications in [29] [31] and [32] are not reconfigurable, though the design in [30] uses a discontinuous reconfigurability technic based on PIN-diodes. Whole, [29] [32] have designs combining two separate structures, while [22] [33] has a relatively large size, with a dimension of the single element patch antenna of $26 \times 24 \text{ mm}^2$ and an overall array size of $(110 \times 110) \text{ mm}^2$ for [22], whereas the dimensions of [33] are $(304 \times 1.7) \text{ mm}^2$.

The simulated results confirm that the performance of the proposed antenna array outperforms in several aspects of our previous work described in [26] and the antennas cited earlier for mmw 5G applications. The reconfigurable antenna array displays proper impedance matching characteristics for the 5G networks based on GT3-23001 LC with continuous controlling bias voltages. The antenna array improvements in widening the bandwidth, increasing the gain, and refinement of the frequency shift are achieved.

4. Conclusion

In this article, An advanced design of 10×1 linear 5G wideband frequency reconfigurable stacked patch antenna array for Ka-band based on GT3-23001 LC as dielectric substrate and aperture coupled feeding is presented. The proposed reconfigurable antenna array acquires the perfect requirements for recent and future mmw 5G networks. The presented single antenna design of the linear array is an optimized design of the compact reconfigurable stacked patch antenna based on GT3-23001 LC through reducing the height of the Rohacell layer from 1 mm to 0.75 mm and by enlarging the width of the patch antenna substrate dimensions from half wavelength over the center frequency to 0.9 of the specified wavelength. These variations over antenna parameters provide improvements over the bandwidth, frequency tunability and antenna gain. Furthermore, the impedance bandwidth of the single antenna element is 8.6 GHz in mmw operating frequency range from 25.3 GHz to 33.8 GHz, corresponding to about 29%, with a continuous frequency shift of 1.18 GHz through controlling the permittivity of the LC with a bias voltage from 0 V to 10.6 V. The antenna array gain between 17.4 dB and 19.2 dB for all the indicated frequency range is achieved with a beamwidth between 4.8° to 6.3° for $\varphi = 0^\circ$. This proposed antenna array design can be a target for future works to improve the tunability and reduce the antenna array dimensions.

Conflicts of Interest

The authors declare no conflicts of interest regarding the publication of this paper.

References

- [1] Deckmyn, T., Agneessens, S., Reniers, A.C.F., Smolders, A.B., Cauwe, M., Ginste, D.V. and Rogier, H. (2017) A Novel 60 GHz Wide-Band Coupled Half-Mode/Quarter-Mode Substrate Integrated Waveguide Antenna Title. *IEEE Transactions on Antennas and Propagation*, **65**, 6915-6926.
<https://doi.org/10.1109/TAP.2017.2760360>
- [2] Jilani, S.F., Member, S., Munoz, M.O. and Abbasi, Q.H. (2017) Millimeter-Wave Liquid Crystal Polymer Based Conformal Antenna Array for 5G Applications. *IEEE Antennas and Wireless Propagation Letters*, **18**, 84-88.
- [3] Rappaport, T.S., *et al.* (2017) Overview of Millimeter Wave Communications for Fifth-Generation (5G) Wireless Networks—With a Focus on Propagation Models. *IEEE Transactions on Antennas and Propagation*, **65**, 6213-6230.
<https://doi.org/10.1109/TAP.2017.2734243>
- [4] Hong, W. (2017) Solving the 5G Mobile Antenna Puzzle: Assessing Future Directions for the 5G Mobile Antenna Paradigm Shift. *IEEE Microwave Magazine*, **18**, 86-102. <https://doi.org/10.1109/MMM.2017.2740538>
- [5] Yashchyshyn, Y., Member, S., Derzakowski, K., Bogdan, G., Member, S., Godziszewski, K., Nyzovets, D., Member, S., Kim, C.H. and Park, B. (2018) 28 GHz Switched-Beam Antenna Based on S-PIN Diodes for 5G Mobile Communications. *IEEE Antennas and Wireless Propagation Letters*, **17**, 2018-2021.
<https://doi.org/10.1109/LAWP.2017.2781262>
- [6] Ouyang, W. and Gong, X. (2018) A Frequency-Reconfigurable Cavity-Backed Slot Antenna ESPAR in H Plane. *IEEE International Symposium on Antennas and Propagation & USNC/URSI National Radio Science Meeting*, Boston, 8-13 July 2018, Vol. 6006, 1917-1918.
<https://doi.org/10.1109/APUSNCURSINRSM.2018.8609292>
- [7] Choi, J., Park, J., Youn, Y., Hwang, W. and Hong, W. (2019) Frequency-Reconfigurable mm Wave Antenna Loaded with Capacitive Structure Integrated within a Microstrip Line. *IEEE International Symposium on Antennas and Propagation and USNC-URSI Radio Science Meeting*, Atlanta, 7-12 July 2019, 455-456.
<https://doi.org/10.1109/APUSNCURSINRSM.2019.8888846>
- [8] Jilani, S.F., Abbas, S.M., Esselle, K.P. and Alomainy, A. (2015) Millimeter-Wave Frequency Reconfigurable T-Shaped Antenna for 5G Networks. *IEEE 11th International Conference on Wireless and Mobile Computing, Networking and Communications (WiMob)*, Abu Dhabi, 19-21 October 2015, 100-102.
<https://doi.org/10.1109/WiMOB.2015.7347946>
- [9] Agarwal, P., Ali, S.N. and Heo, D. (2017) Reconfigurable Phased-Array Design Techniques for 5G and Beyond Communications. *IEEE International Symposium on Radio-Frequency Integration Technology (RFIT)*, Seoul, 30 August-1 September 2017, 53-55. <https://doi.org/10.1109/RFIT.2017.8048287>
- [10] Yi, Y., Yong, C., King Yuk, C., Ramer, R. and Guo, Y.J. (2011) MEMS-Loaded Millimeter Wave Frequency Reconfigurable Quasi-Yagi Dipole Antenna. *Asia-Pacific Microwave Conference*, Melbourne, 1318-1321.
- [11] Perez-Palomino, G., Encinar, J.A., Barba, M., Cahill, R., Dickie, R. and Baine, P. (2018) Millimeter-Wave Beam Scanning Antennas Using Liquid Crystals. *9th European Conference on Antennas and Propagation (EuCAP)*, Lisbon, 4.
- [12] Barbin, S., da Costa, I., Cerqiera Sodre Junior, A., Spadoti, D., da Silva, L.G. and Ribeiro, J.A. (2017) Optically Controlled Reconfigurable Antenna Array for mm-Wave Applications. *IEEE Antennas and Wireless Propagation Letters*, **16**,

- 2142-2145. <https://doi.org/10.1109/LAWP.2017.2700284>
- [13] Maune, H., Jost, M., Reese, R., Polat, E. and Nickel, M. (2018) Microwave Liquid Crystal Technology. *Crystals*, **8**, 355. <https://doi.org/10.3390/cryst8090355>
- [14] Langley, R.J. and Liu, L. (2008) Liquid Crystal Tunable Microstrip Patch Antenna. *Electronics Letters*, **44**, 1179-1180. <https://doi.org/10.1049/el:20081995>
- [15] Fritsch, C., Bildik, S. and Jakoby, R. (2012) Ka-Band Frequency Tunable Patch Antenna. *Proceedings of the 2012 IEEE International Symposium on Antennas and Propagation*, Chicago, 8-14 July 2012, 1-2. <https://doi.org/10.1109/APS.2012.6348462>
- [16] Oliver, D.R. and Schaub, D.E. (2011) A Circular Patch Resonator for the Measurement of Microwave Permittivity of Nematic Liquid Crystal. *IEEE Transactions on Microwave Theory and Techniques*, **59**, 1855-1862. <https://doi.org/10.1109/TMTT.2011.2142190>
- [17] Goelden, F., Gaebler, A., Karabey, O., Goebel, M., Manabe, A. and Jakoby, R. (2010) Tunable Band-Pass Filter Based on Liquid Crystal. *German Microwave Conference Digest of Papers*, Berlin, 15-17 March 2010, 98-101.
- [18] Weil, C., Luessem, G. and Jakoby, R. (2002) Tunable Inverted-Microstrip Phase Shifter Device Using Nematic Liquid Crystals. *IEEE MTT-S International Microwave Symposium Digest*, Seattle, 2-7 June 2002, Vol. 1, 367-370.
- [19] Nestoros, M., Papanicolaou, N.C. and Polycarpou, A.C. (2019) Design of Beam-Steerable Array for 5G Applications Using Tunable Liquid-Crystal Phase Shifters. *13th European Conference on Antennas and Propagation (EuCAP)*, Krakow, 31 March-5 April 2019, 1-4.
- [20] Yaghmaee, P., Kaufmann, T., Bates, B. and Fumeaux, C. (2012) Effect of Polyimide Layers on the Permittivity Tuning Range of Liquid Crystals. *6th European Conference on Antennas and Propagation (EuCAP)*, Prague, 26-30 March 2012, 3579-3582. <https://doi.org/10.1109/EuCAP.2012.6205944>
- [21] Jung, Y. and Diawuo, H.A. (2018) Broadband Proximity-Coupled Microstrip Planar Antenna Array for 5G Cellular Applications. *IEEE Antennas and Wireless Propagation Letters*, **17**, 1286-1290. <https://doi.org/10.1109/LAWP.2018.2842242>
- [22] Ikram, M., Nguyen-trong, N. and Abbosh, A. (2019) Patch Antenna Array with Continuous Frequency and Polarization Tuning for 5G Mid-Band Communications. *IEEE International Symposium on Antennas and Propagation and USNC-URSI Radio Science Meeting*, Atlanta, 7-12 July 2019, 911-912. <https://doi.org/10.1109/APUSNCURSINRSM.2019.8888876>
- [23] Parchin, N.O., Basherlou, H.J., Al-yasir, Y.I.A., Ullah, A., Abd, R.A., Noras, J.M., Bd, B., College, B. and Yorkshire, W. (2019) Frequency Reconfigurable Antenna Array with Compact End-Fire Radiators for 4G/5G Mobile Handsets. *2019 IEEE 2nd 5G World Forum*, Dresden, 30 September-2 October 2019, 204-207. <https://doi.org/10.1109/5GWF.2019.8911707>
- [24] Parchin, N.O., et al. (2019) Recent Developments of Reconfigurable Antennas for Current and Future Wireless Communication Systems. *Electronics Letters*, **8**, 1-17. <https://doi.org/10.3390/electronics8020128>
- [25] Zainarry, S.N.M., Nguyen-Trong, N. and Fumeaux, C. (2018) A Frequency and Pattern-Reconfigurable Two-Element Array Antenna. *IEEE Antennas and Wireless Propagation Letters*, **17**, 617-620. <https://doi.org/10.1109/LAWP.2018.2806355>
- [26] El-Hassan Hajj, A., Fadlallah, N., El-Nashef, G., Rammal, M. and Rachid, E. (2019) Compact Reconfigurable Stacked Patch Antenna Using Liquid Crystal for 5G Networks. *2nd IEEE Middle East and North Africa Communications Conference*

- (*MENACOMM*), Manama, 19-21 November 2019, 2-5.
- [27] Evonik (2011) Dielectric Properties ROHACELL®. 1-3.
- [28] Ikram, M., Al Abbas, E., Nguyen-trong, N., Sayidmarie, K.H. and Abbosh, A. (2019) Integrated Frequency-Reconfigurable Slot Antenna and Connected Slot Antenna Array for 4G and 5G. *IEEE Transactions on Antennas and Propagation*, **67**, 7225-7233. <https://doi.org/10.1109/TAP.2019.2930119>
- [29] Lee, C., Khattak, M.K. and Kahng, S. (2018) Wideband 5G Beamforming Printed Array Clutched by lte-a 4x4 Multiple-Input-Multiple-Output Antennas with High Isolation. *IET Microwaves, Antennas & Propagation*, **12**, 1407-1413. <https://doi.org/10.1049/iet-map.2017.0946>
- [30] Al Abbas, E., Member, S., Nguyen-trong, N. and Toaha, A. (2019) Polarization-Reconfigurable Antenna Array for Millimeter-Wave 5G. *IEEE Access*, **7**, 131214-131220. <https://doi.org/10.1109/ACCESS.2019.2939815>
- [31] Ikram, M., Sharawi, M.S., Shamim, A. and Shamim, A. (2018) A Multiband Dual-Standard MIMO Antenna System Based on Monopoles (4G) and Connected Slots (5G) for Future Smart Phones. *Microwave and Optical Technology Letters*, **60**, 1468-1476. <https://doi.org/10.1002/mop.31180>
- [32] Hussain, S. R., Alreshaid, A.T., Podilchak, S.K. and Sharawi, M. (2017) Compact 4G MIMO Antenna Integrated with a 5G Array for Current and Future Mobile Handsets. *IET Microwaves, Antennas & Propagation*, **11**, 271-279. <https://doi.org/10.1049/iet-map.2016.0738>
- [33] Sharawi, M.S., Ikram, M. and Shamim, A. (2017) A Two Concentric Slot Loop Based Connected Array MIMO Antenna System for 4G/5G Terminals. *IEEE Transactions on Antennas and Propagation*, **65**, 6679-6686. <https://doi.org/10.1109/TAP.2017.2671028>